*Environment and Planning B: Planning and Design* 2006, volume 33, pages 39 – 58

DOI:10.1068/b31195

# Assessment of urban environmental quality in a subtropical city using multispectral satellite images

**Janet Nichol, Man Sing Wong**
Department of Land Surveying and Geo-Informatics, The Hong Kong Polytechnic University, Hunghom, Kowloon, Hong Kong; e-mail: lsjanet@polyu.edu.hk

**Christopher Fung, Kenneth K M Leung**
Air Modelling Section, Environmental Protection Department, 33F Revenue Tower, Wan Chai, Hong Kong; e-mail: kleung@epd.gov.hk
Received 17 October 2003; in revised form 5 February 2005

**Abstract.** Urban environmental quality (UEQ) is a complex and spatially variable parameter of increasing concern, especially in densely populated cities of the tropics and subtropics where climate, air quality, and the urban infrastructure may interact to produce uncomfortable and hazardous effects. The study investigates the application of multispectral remote sensing from the Landsat ETM+ and IKONOS satellite sensors for the mapping of UEQ in urban Hong Kong at a detailed level, using the measurable, image-based parameters of temperature and biomass, and examines the relationship between these and air quality in selected study districts. Multiple-criteria queries on these two parameters show that spatial variations in UEQ are closely related to natural topographic factors and urban morphology. The amount of biomass, as opposed to total area of vegetation, is also shown to be an important factor in the spatial variation of UEQ. The data permit visualisation of the relationship between the human and natural factors involved in UEQ and generate recommendations for future planning and urban-renewal projects.

## Introduction

With a high-rise living environment for over 90% of the population and plot ratios of up to 55 000 persons per $km^2$ Hong Kong's urban areas are the most densely populated in the world. Recent perceptions of an unhealthy and stressful living environment emphasised by the recent SARS (Severe Acute Respiratory Syndrome) epidemic, have led to demands for the improvement of urban environmental quality (UEQ) including more, and better distributed green spaces in the city. Some areas such as Mongkok and ShamShuiPo in Kowloon, and Causeway Bay on Victoria Island are notorious for their poor environmental quality, including congestion, high air pollution levels, heat, and noise. Both Mongkok and Causeway Bay far exceeded the compliance status in annual average levels of nitrogen dioxide ($NO_2$) and respirable suspended particulates (RSP) in 2001 and their mean annual air pollution indices are classed as 'high' (Environmental Protection Department, 2004). Although opinion polls most often cite air quality as being of greater concern than other variables such as green space and ambient air temperature, in most cities there are two few air quality monitoring stations to use this as a spatially distributed indicator of UEQ (Akbari et al, 1990). As green vegetation is an important indicator of UEQ (Emmanuel, 1997) a method is described to derive accurate maps of biomass amount from high resolution IKONOS images and to relate these to air quality and to another index of UEQ, the urban heat island (UHI), derived from Landsat Enhanced Thematic Mapper+ (ETM+) thermal imagery. A major constraint on the use of remote sensing for assessment of UEQ is the inability to sense air quality directly at a detailed level. However, there have been many references to the relationship between air pollution and biomass on the one hand (Dwyer et al, 1992) and air pollution and the UHI on the other (Klaus et al, 1999). The use of remote sensing imagery for such a study is in many ways superior to

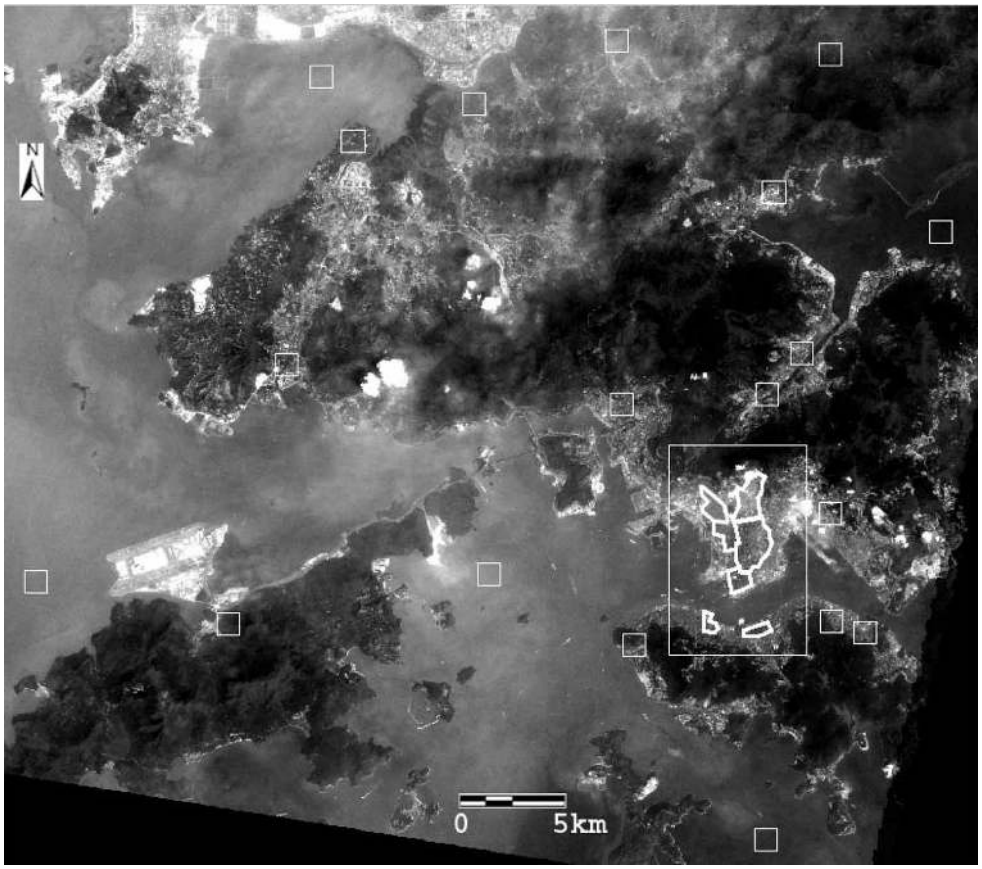


**Figure 1.** Landsat ETM+ image of Hong Kong showing the positions of the study districts in Kowloon Peninsula in the area covered by the IKONOS image (rectangle). Squares correspond to sample pixels of air quality model data.

field-based techniques because environmental quality is a spatially variable and complex parameter, but is usually measured at points: for example, climatic and air pollution indices are measured at fixed stations and urban biomass, if quantified at all, is usually measured by inventories of individual street trees.

The study concentrates on seven urban districts in Hong Kong (figure 1), four of which were selected for consistently having high levels of air pollution, and a further three districts where air pollution levels are not noted to be high. The spatially detailed nature of the imagery enables assessment of temperature and biomass at the level of the individual street or city block.

## Objectives

This study presents a method for UEQ mapping and assessment at a detailed level which combines two types of remotely sensed image data. These are a map of biomass amount derived from a 4 m resolution multispectral IKONOS image, and a map of surface temperature used as a surrogate for ambient air temperature, derived from a Landset ETM+ image and fused with IKONOS to give a 4 m pixel size.

The aim of the projects are

(1) to use remote sensing methods to obtain empirical measurements of the amount of biomass and heat island intensity for seven urban districts in Hong Kong;

(2) to note any relationship between these two parameters, and between them and air pollution indices; thus
(3) to assess the extent to which UEQ can be mapped and evaluated using remote sensing data.

**Remote sensing of urban vegetation**

Traditional methods of mapping urban vegetation combine colour infrared aerial images and fieldwork. Common parameters measured by air photograph interpretation include the total green space and the percentage of tree canopy space as a proportion of the total (Nowak et al, 1996). In Hong Kong the Environment, Transport and Works Bureau maintains over 500 000 records of urban trees and the urban and rural planning authorities have a new experimental policy of acquiring large-scale, false colour infrared aerial photographs for environmental monitoring. Although such methods are expensive and time consuming and require periodic updates to remain valid they have until recently been the only option because medium resolution satellite images such as SPOT and Landsat (Barnsley and Barr, 1996; Gao and Skillcorn, 1998) lack the necessary spatial detail to detect the often fragmented vegetation cover of urban areas, such as a single row of street trees or a grassy road verge. However, Landsat imagery was used by Fung and Siu (2001) to conduct a survey of green space in Hong Kong as an index of environmental quality at the generalised level of the tertiary planning unit. They used the normalised difference vegetation index (NDVI), obtaining a mean value for each unit and assessing changes over time. As in many cases in which the NDVI is used for representing vegetation it was selected on the basis of its perceived robustness in a wide variety of situations and to represent a variety of parameters such as vegetation cover, biomass, leaf area index (LAI), vegetation vigour, and for visualisation (Curran, 1980; Lawrence and Ripple, 1998). These perceptions are often based on previous studies carried out in other study areas using different sensing systems, and do not usually demand or produce any mathematical relationship between the NDVI and vegetation amount. Moreover, when used as an indicator of the presence or absence of vegetation (that is, vegetation cover), placing of the threshold is necessarily subjective. The same problems attend the use of other standard vegetation indices such as the Kauth – Thomas greenness index as a socioeconomic indicator in Detroit (Emmanuel, 1997).

In theory the green:red ratio should be a better indicator of vegetation than the NDVI in urban areas because, according to Colwell (1974), when the background is light and leaf area low, the negative relationship between LAI and the red wavelengths may be stronger than the positive relationship between the LAI and the near infrared (NIR) wavelengths, because both the vegetation and the background are highly reflecting in the NIR region.

**Quantifying vegetation amount from IKONOS**

A multispectral IKONOS image was acquired by Space Imaging Inc. on 23 November 2000, having a spatial resolution of 4 m in four wavebands and with an off-nadir look angle of 19°. It covers the whole of Kowloon Peninsula and the northern part of Hong Kong Island (figure 1). A model was developed (Nichol and Lee, 2005) to quantify urban vegetation by comparing the IKONOS image bands with forty-one vegetation plots measured in the field. The plots were measured by using the line intersect method whereby vegetation in 16 $m^2$ quadrats is recorded by cover and structural type along five traverses across the quadrat (Hanley, 1978).

Because the environmental importance of vegetation in urban areas may be related less to the area covered by vegetation than to the total amount of biomass, the parameter vegetation density (VD) was devised to measure vegetation amount in all vertical

layers above ground. It is a substitute for the commonly used LAI (Curran, 1983) which is defined as the cumulative, one-sided leaf area per unit ground area. VD was computed according to:

$$\%\,\mathrm{VD} \;=\; 100\frac{W_v L_v}{L}\Big/\sum_v W_v\,, \tag{1}$$

where

$W_v$ is the weighting for each vegetation structural type $v$;

$L_v$ is the length covered by vegetation type $v$;

$L$ is the total length in plot.

Weightings for vegetation types were given as in table 1. Thus VD differs from another commonly used vegetation parameter, vegetation cover (VC), which refers to the percentage of ground covered by vegetation (table 2). All vegetated areas have a value for VD, but the value may be low if biomass is low: thus a plot with 100% VC of short grass (for example, a football pitch) would have a VD value of 9.5%, but a fairly well-vegetated forest plot having 90% VC of tall trees, 30% shrub, and 50% tall grass would have a VD value of 46% (table 2).

**Table 1.** Weightings allocated to structural vegetation types for vegetation density.

| Type | Weighting | Description |
|---|---|---|
| Short grass | 0.2 | Green grass lower than 0.5 m |
| Tall grass | 0.3 | Green grass higher than 0.5 m |
| Shrub | 0.4 | Short and woody plant with woody (nongreen) stems from the base |
| Small tree | 0.5 | Woody plant with trunk diameter $<$0.3 m |
| Large tree | 0.7 | Woody plant with trunk diameter $>$0.3 m |

**Table 2.** Comparison of values recorded for two vegetation parameters.

| Vegetation types in plot | Vegetation cover | Vegetation density |
|---|---|---|
| Well vegetated: 90% tall tree, 30% shrub, 50% grass | 90–100 | 46 |
| Football pitch: 100% short grass | 100 | 9.5 |
| Waste ground: 30% shrub, 40% grass | 40–70 | 14 |
| Street tree, crown occupying full pixel: 100% tall tree | 100 | 33 |

Shadows were removed from images by radiometric masking in the NIR band. Following this, the best band combination to represent VD was the green:red ratio, with an $R^2$-value of 0.80 (that is, explaining 80% of the data variability) and this was better than the $R^2$-value of 0.61 obtained from the use of the NDVI. An accuracy test comparing the percentage VD to the forty field-measured quadrats with a map of VD produced from the regression equation,

$$\mathrm{VD} \;=\; 1.657(1000X^{\frac{1}{2}}) - 404.443X + 34.873\,, \tag{2}$$

(where $X$ is the IKONOS green:red ratio) showed a mean difference of only 4.1%. The same mapping undertaken using large-scale (1:8000) false colour aerial photographs of the study area, Kowloon Peninsula (Nichol and Lee, 2005) did not produce significantly higher accuracy. Therefore, the higher cost-effectiveness of IKONOS in terms of reduced image-processing time for a single mapping base, as well as the absolute radiometric calibration available for satellite images, recommends it over aerial photographs for automated vegetation mapping in urban areas at detailed level.

Colour plates 1(a) and 1(b) (over) show a false colour composite of ETM+ green and red bands displayed as blue and green, and with VD and VC from IKONOS displayed as red, overlaid with the district boundaries. For a full critique of the method see Nichol and Lee (2005).


**Figure 2.** Grey-level sliced thermal image; temperatures in degrees Celsius.

**Remote sensing of urban microclimate**

Hong Kong has hot summers in which heat loading is a concern for the human bioclimate. Recent statements (*South China Morning Post* 2002) suggest that Hong Kong has a well-developed, and increasing UHI with a magnitude of 3 – 5°C, centred on the Kowloon Peninsula. The morning timing of Landsat is not optimal for sensing the urban heat island, which is more pronounced at night. However, distinct microclimatic patterns precursory to UHI development are evident on the images (figure 2), and the relevance of this approach to urban planning has been demonstrated (Nichol, 1994; 1996; 2005). Several satellite-based studies of urban climate have claimed a strong association between two image-derived parameters, surface temperature and biomass, the latter represented by the NDVI (Gallo et al, 1993a; 1993b; Lo et al, 1997; Weng, 2001) and the work of Carlson and Boland (1978), on the relationship between moisture availability, surface roughness, and surface temperature, is often cited. Gallo et al even maintain that a vegetation index such as the NDVI from the National Oceanic and Atmospheric Administration, Advanced Very High Resolution Radiometer satellite sensor is a superior indicator of the UHI than is surface temperature derived from the same sensor. Thus biomass indicators could be used as a surrogate for temperature if thermal data are unavailable or if there is inadequate spatial resolution. In cases such as Hong Kong, where cool shady places and small pockets of greenery within the congested inner city are of immense environmental importance, it is necessary to measure temperature and biomass accurately and at detailed level, or if one can be measured accurately it can be used to supplement the other. This study uses the biomass index VD developed from fine (4 m) resolution multispectral IKONOS imagery discussed above, to enhance the lower (60 m) resolution thermal image data from Landsat ETM+.

**Deriving surface and air temperature from Landsat ETM+**

The ETM+ image covers almost the whole of Hong Kong, and was acquired on 17 September 2001, less than one year following the IKONOS image data (figure 1). The thermal band of the EMT+ image was geometrically corrected. It was also corrected for atmospheric factors and differential emissivity of land-cover types and converted to surface temperature ($T_s$) by the procedures described in the appendix. Figure 2 shows the corrected $T_s$ values which range from approximately 29° to 41°C. The $T_s$ image pixel size after emissivity correction (appendix) using the IKONOS image was 4 m and this enabled the combination of data from each sensor as separate bands of the same file for purposes of statistical analysis and visualisation by multicriteria querying. The bands and band combinations are given in table 3. Previous studies (Ben-Dor and Saaroni, 1997; Nichol, 1996) have established a strong relationship between $T_s$ and the temperature of the adjacent air ($T_a$), suggesting that the satellite-derived $T_s$ is a relevant indicator of the UHI. This was also tested in the present study using contact thermistors and a noncontact thermometer with 545 data pairs, over a variety of surface materials at the surface and at a height of 1 m above it. The correlation coefficient between $T_s$ and $T_a$ was 0.97 for the hourly averages.

**Table 3.** Bands combined into a six-band file, having 4 m pixel size.

| Landsat ETM+ | IKONOS |
|---|---|
| Normalised difference vegetation index (NDVI) | vegetation cover (VC) |
| green:red ratio | vegetation density (VD) |
| $T_s$ | |
| $T_a$ | |

**Air quality parameters**

Establishing a relationship between the image-based parameters and an additional important parameter of UEQ, air quality, is difficult because of the problems of comparing point data from air quality monitoring stations with raster image data, as well as the fact that only three districts in the present study measure air quality. Therefore, modelled air quality data covering Hong Kong and the Pearl River Delta region were used. These data in 1.5 $km^2$ raster format (Fung et al, 2003) are based on a large number of known emission sources across Hong Kong and the neighbouring Pearl River Delta, combined with synchronous meteorological parameters. The model data have been continuously improved over the last two years and are known to compare favourably with data at the fourteen monitoring stations in Hong Kong and thirty stations in the Pearl River Delta. Thirty sample pixels from the model data (shown on figure 1 overlain on the Landsat image) were correlated with the image-derived temperature ($T_s$). For the seven urban districts covered by the IKONOS image (figure 1), both $T_s$ and VD were tested against the modelled air quality. The data and correlations for the seven urban districts are given in table 4 (over) .

**Results**

The districts of Mongkok, ShamShuiPo, and Causeway Bay appear to be almost totally unvegetated and Mongkok and ShamShuiPo are also the warmest. HoManTin is the best vegetated district (colour plate 1) and also the coolest (table 4). Within the districts, $T_s$ from ETM+ was found to be highly correlated with biomass (VD) from IKONOS ($R^2 = 0.82$) (table 4 and figure 3, over). This conforms to the previous findings of Carlson and Boland (1978). This correlation was also found to be higher than that obtained between $T_s$ and the NDVI, both from EMT+ ($R^2 = -0.79$). Because VD was obtained from the IKONOS green:red ratio and in view of the difference in spatial resolution between the two sensors this may be surprising, but it provides support for the effectiveness of this ratio as a quantitative measure of biomass amount.

In order to visualise UEQ as a spatial parameter, two assumptions were made: first that UEQ is inversely correlated with the UHI and directly correlated with biomass amount; second that the two parameters, biomass and temperature, operate as independent indices of UEQ. Multicriteria queries were performed based on standard deviation (SD) as the threshold. Thus query A selects pixels having $T_s$ above 1.5 SD and VD below 1.5 SD of the mean and returns the areas of lowest UEQ according to the two criteria (warm areas with little vegetation) (figure 4, over)

*Query A*: if $T_s > 38^{\circ}$C, and VD $< 5\%$, then $q_1$; else null,

where $q_1$ is the quality value of the query (for example, areas of lowest UEQ).

The poorest air quality areas within the study districts were seen to be in ShamShuiPo and northwest Mongkok, particularly in areas with a well-defined northwest – southeast-oriented street pattern parallel to the sun azimuth at the image time (figure 5, over). Areas with a north – south street orientation are not returned. Considering the whole image, areas of low UEQ are on the periphery of Kowloon Peninsula, around the coast. They occupy reclaimed land and are either currently barren or have low-rise development with a high sky view factor (SVF) such as the old Kai Tak airport, railway and transport routes, markets, and port and warehouse facilities.

However because some warm areas do have significant amounts of vegetation, and some cool areas are unvegetated or sparsely vegetated, it is informative to examine

**Table 4.** Air quality and image parameters in the urban study districts (model air quality data for 10am on 17 September 2001).

| | Building type (rise: high/low/medium) | $NO_2$ ($\mu g/m^3$) | $NO_x$ ($\mu g/m^3$) | $O_3$ ($\mu g/m^3$) |
|---|---|---|---|---|
| Causeway Bay | High rise | 49.4 | 61.7 | 24.5 |
| Mongkok | Medium rise | 54.8 | 73.1 | 22.7 |
| ShamShuiPo | Medium rise | 52.4 | 64.6 | 26.1 |
| HoManTin | Medium rise | 50.7 | 69.4 | 21.3 |
| Kowloon Tong | Low/medium | 42.6 | 60.5 | 20.1 |
| Central/Western | Medium rise | 52.3 | 68.1 | 22.9 |
| TsimShaTsui | Medium rise | 51.4 | 65.6 | 24.5 |
| Correlation with $T_s$ | | 0.81* | 0.72* | −0.30 |
| Correlation with VD | | −0.29 | 0.11 | −0.61 |

* Significant at 5% confidence level, DF = 6.

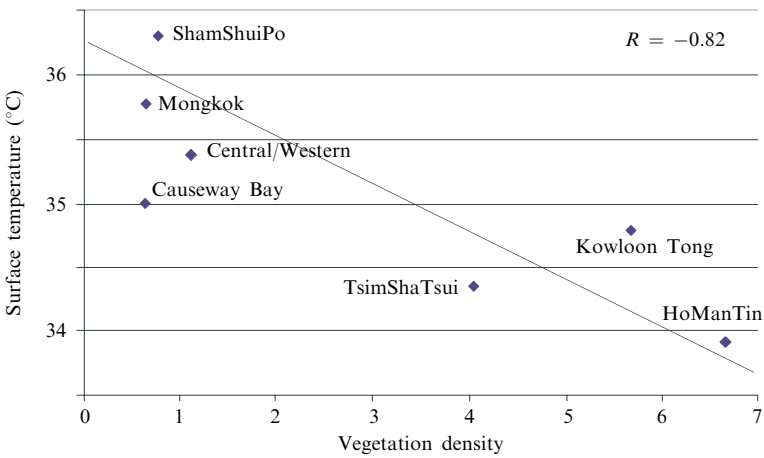


**Figure 3.** Relationship between surface temperature ($T_s$) and vegetation density (VD).

the residuals. Thus

*Query B*: if $T_s > 38°C$, and VD > 5%, then $q_1$; else null.

Query B returns those areas which are both warm and vegetated. Over the whole image these areas comprise mainly grassed areas, such as sports grounds, the race-course, the margins of the airport runway, and reclaimed waste ground [figure 6(a)]. This suggests the inability of open grassy surfaces to moderate the local temperature. Accordingly, in a study of the climate of urban parks, Spronken-Smith and Oke (1998) found that unirrigated grass parks (as opposed to treed parks) within cities are unable to establish a daytime park cool island (PCI) thanks to the high SVF, especially if soils are dry, having low thermal admittance. In the present study, the eight days previous to the image date had been extremely dry, with a total of only 7.5 mm rainfall. On the other hand, irrigated parks as well as those with treed borders were able to establish a substantial PCI. Victoria Park adjacent to Causeway Bay is irrigated and has treed borders, and does not satisfy query B although it has substantial grassy areas. It is relatively cool, being approximately 4°C cooler than the high-rise district of Causeway Bay (colour plate 3).

**Table 4** (continued).

| | $SO_2$ ($\mu g/m^3$) | RSP ($\mu g/m^3$) | Mean image $T_s$ | Mean image VC | Mean image VD |
|---|---|---|---|---|---|
| Causeway Bay | 22.5 | 129.1 | 35.0 | 4.6 | 0.6 |
| Mongkok | 18.4 | 136.9 | 34.9 | 4.8 | 0.6 |
| ShamShuiPo | 18.8 | 133.8 | 36.3 | 5.2 | 0.8 |
| HoManTin | 17.8 | 135.4 | 33.9 | 32.8 | 6.7 |
| Kowloon Tong | 12.6 | 134.6 | 34.8 | 30.3 | 5.7 |
| Central/Western | 24.0 | 129.7 | 34.9 | 5.4 | 1.1 |
| TsimShaTsui | 19.9 | 132.3 | 34.6 | 9.1 | 3.5 |
| Correlation with $T_s$ | 0.70* | 0.69* | | | |
| Correlation with VD | −0.68* | 0.41 | | | |

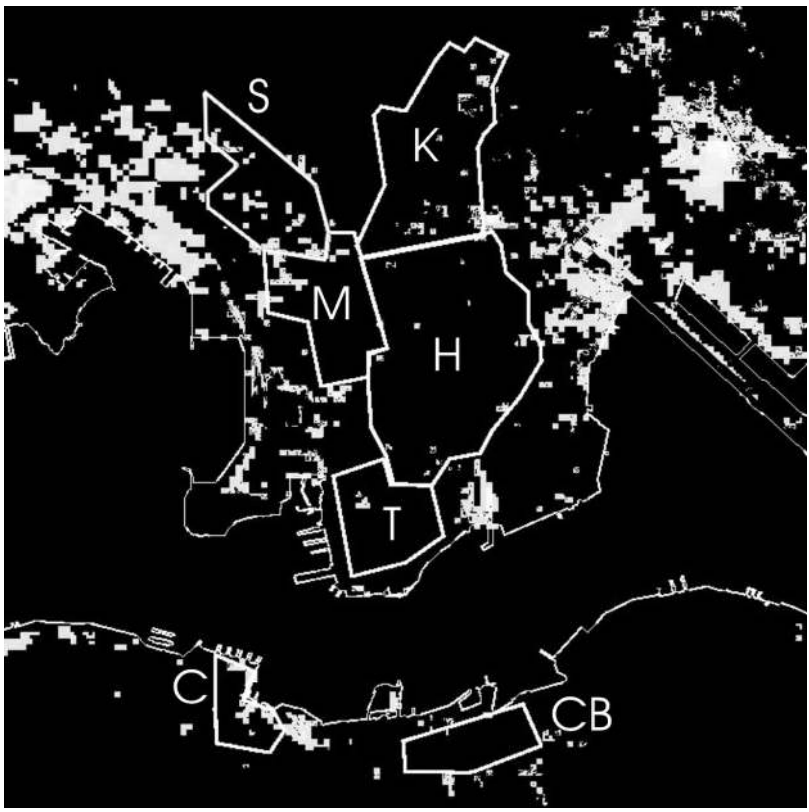


**Figure 4.** Query A: areas with lowest urban environmental quality C = Central/Western, CB = Causeway Bay, H = HoManTin, K = Kowloon Tong, M = Mongkok, S = ShamShuiPo, T = TsimShaTsui.

Query C is concerned with areas which, although little vegetated, remain cool, with 'cool' defined as <1.5 SD below mean $T_s$:

*Query C*: if $T_s < 32^{\circ}$C, and VD < 5%, then $q_1$; else null.

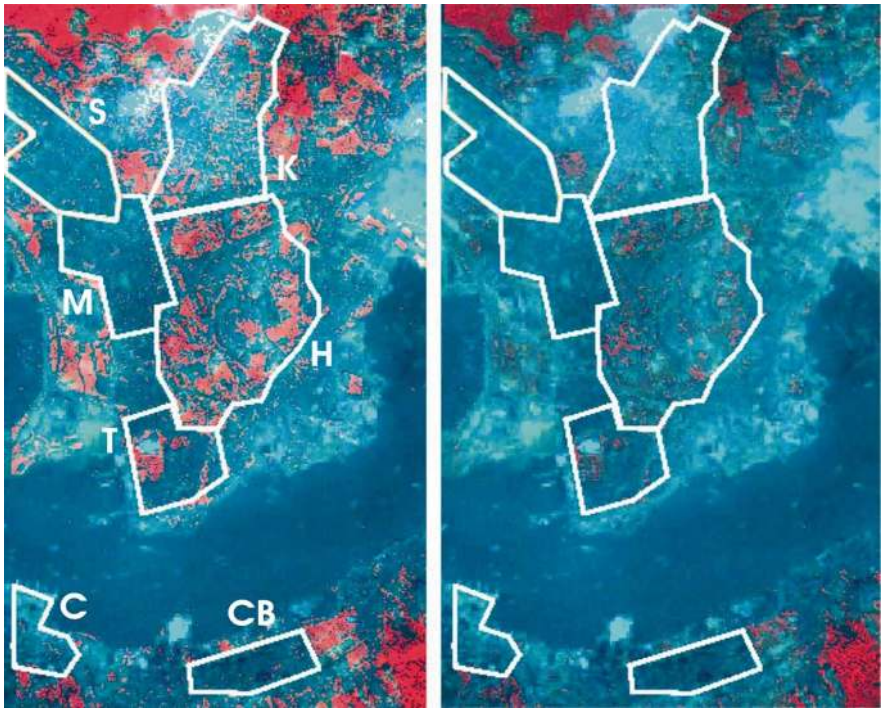


(a) (b)

**Colour plate 1.** False colour composite of vegetation cover (VC) and vegetation density (VD) combining ETM+ bands 2 and 3 on blue and green, and IKONOS VD and VC, respectively, on red display: (a) VC which records only presence or absence displays as bright red. District boundaries overlaid; (b) VD represents a range of biomass amount and displays as a range of pink to red. C = Central/Western, CB = Causeway Bay, H = HoManTin, K = Kowloon Tong, M = Mongkok, S = ShamShuiPo.

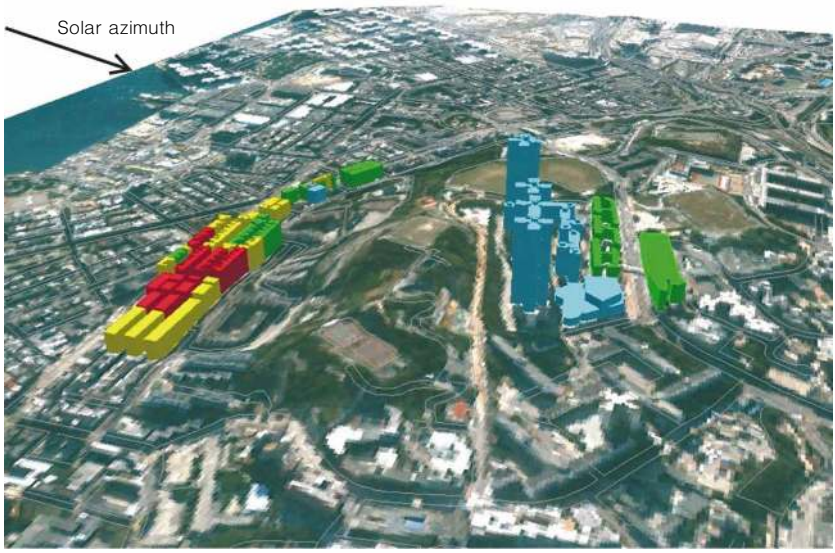


(a)

**Colour plate 2.** Terrain model of HoManTin looking south over Kowloon Peninsula (a) model overlain with IKONOS image: selected buildings on sunny and shady side of inselberg extruded to actual height, with colour according to image-drived surface temperature $T_s$ (b) model overlain with $T_s$ image (temperatures in °C).

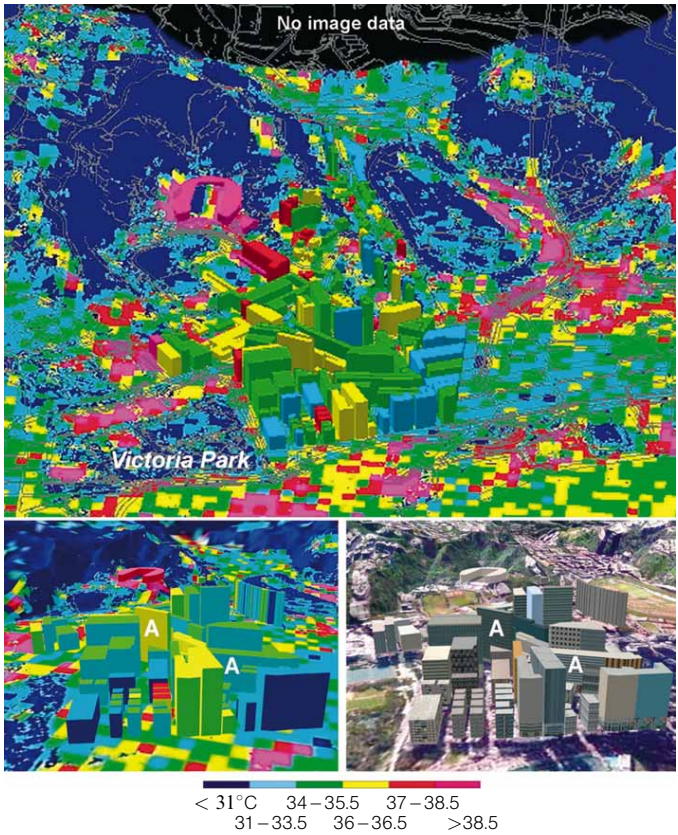


**Colour plate 3.** Terrain model looking north across Victoria Harbour, to the shoreline at Causeway Bay. Upper and lower left figures show selected buildings extruded to actual height, coloured according to image-drived surface temperature, $T_s$. Lower right represents model overlain with IKONOS image. Buildings blocking fresh air corridors are labeled 'A'.

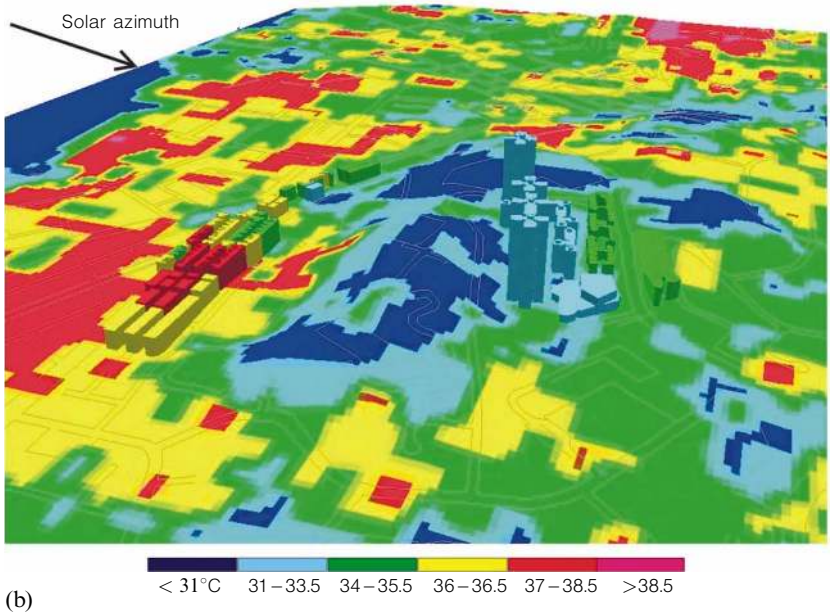


(b)

**Colour plate 2** (continued).

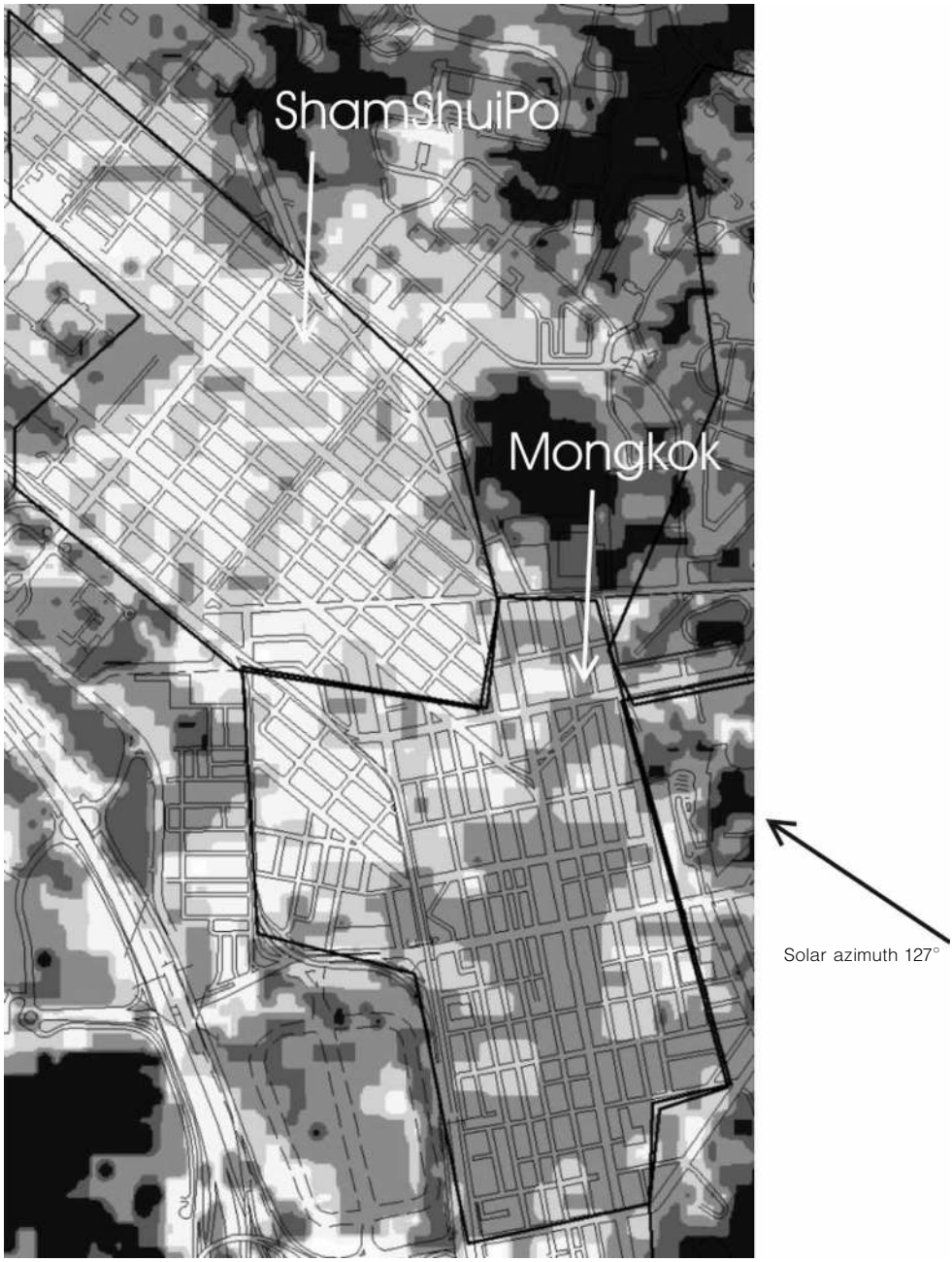


**Figure 5.** Landsat colour classified thermal image overlaid with street vector layer showing the correspondence between surface temperature and street orientation in ShamShuiPo and Mongkok districts. Legend as for figure 2.

Within the study districts this returns small patches created by a low sun angle and azimuth on slopes, the shadows of tall buildings and areas adjacent to pockets of vegetation in the well-vegetated HoManTin district [figure 6(b)]. Over the whole image, the sea surface is the main cool but unvegetated area. However, whereas many cool low vegetated areas are seen to be adjacent to well-vegetated patches, suggesting some

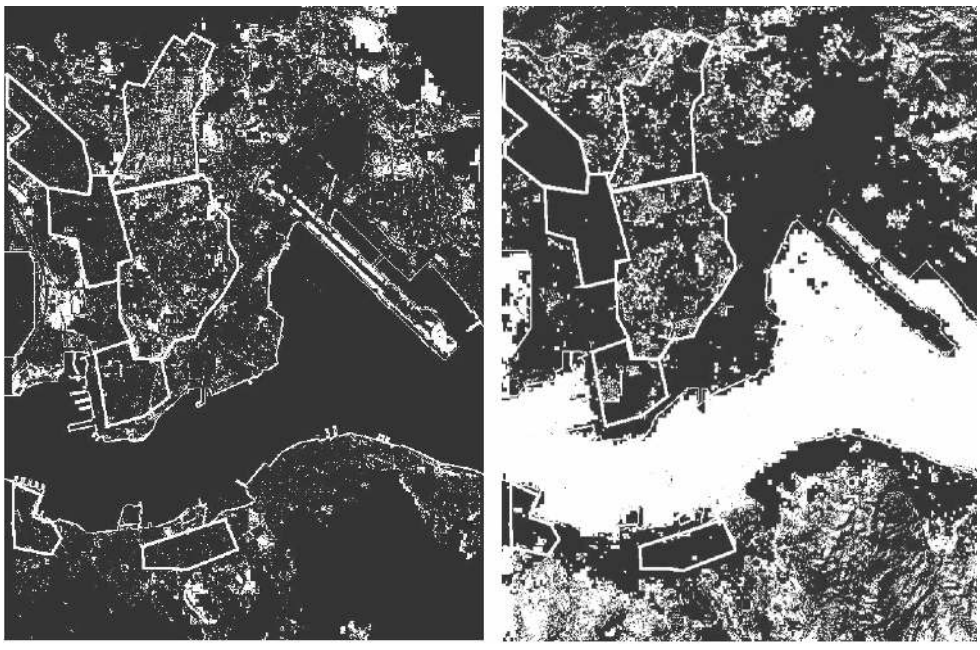

(a) (b)

**Figure 6.** (a) Query B: warm but vegetated areas; (b) query C: cool but unvegetated areas.

microadvection, no areas around the almost totally unvegetated coastline fall into this category, suggesting little microadvection from the water surface. Furthermore, no coastal land areas fall into the cool category with temperatures less than 32°C. These observations suggest that proximity to the sea alone does not provide a cooling effect, and that tree vegetation, which satisfies Carlson and Boland's (1978) criteria for surface cooling (high moisture availability and surface roughness), as well as providing shade, is required to moderate temperature at the coast.

Apart from the sea surface, the most extensive area which is both low vegetated and cool is found in HoManTin district (H on figure 4), on the shaded side of a steep, wooded inselberg. This western side of the inselberg supports two rows of high-rise residential buildings built along the slope contour, the upslope building over 100 m high. The two deep canyons created by these remain in shadow at the image time and are 8°C cooler than low-rise areas which are similarly unvegetated (colour plate 2, page 10 – 11). However, this shaded area, at 31°C, is still 2° warmer than the adjacent woodland and is the same temperature as two grassed football pitches nearby.

Also it is notable that, although the area of Mongkok with a north – south street orientation is not among the warmest areas, neither is it among the coolest and does not satisfy query C (low vegetated but cool). Thus although the low SVF due to the medium-rise buildings may delay heating, this area is already moderately warm in the early morning. As the sun angle increases and as the solar azimuth becomes more southerly it would lose this advantage later in the day.

*Query D*: if $T_s < 36$°C, and VD $> 5$%, then $q_1$; else null,

returns areas of highest UEQ which are cool and vegetated. These areas include not only extensive areas on the urban periphery and urban treed parks, but also, thanks to the 4 m pixel size after emissivity correction, small pockets of dense greenery as found

**Figure 7.** Small treed public park in Mongkok.

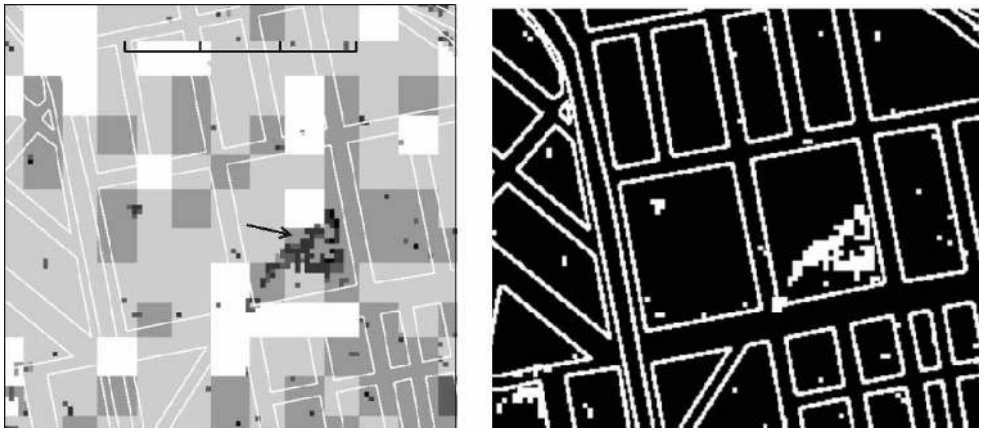

(a) (b)

**Figure 8.** Images of park (arrowed) shown in figure; (a) grey-level sliced surface temperatures, $T_s$ (after emissivity correction using 4 m pixels of IKONOS vegetation density image): legend as for figure 2; (b) return of query D—cool vegetated areas.

in small treed parks within highly built areas such as Mongkok and ShamShuiPo (figures 7 and 8).

**Relationship between the parameters of urban environmental quality**

Correlations between data collected at the same points over a time series are usually high, as shown by figure 9 for the daily temperature and air pollution index at Mongkok for the month of the ETM+ image, September 2001, with a correlation coefficient of 0.84. The Hong Kong Environmental Protection Department (2004) recognises a spatial relationship between mesoscale climatological factors which

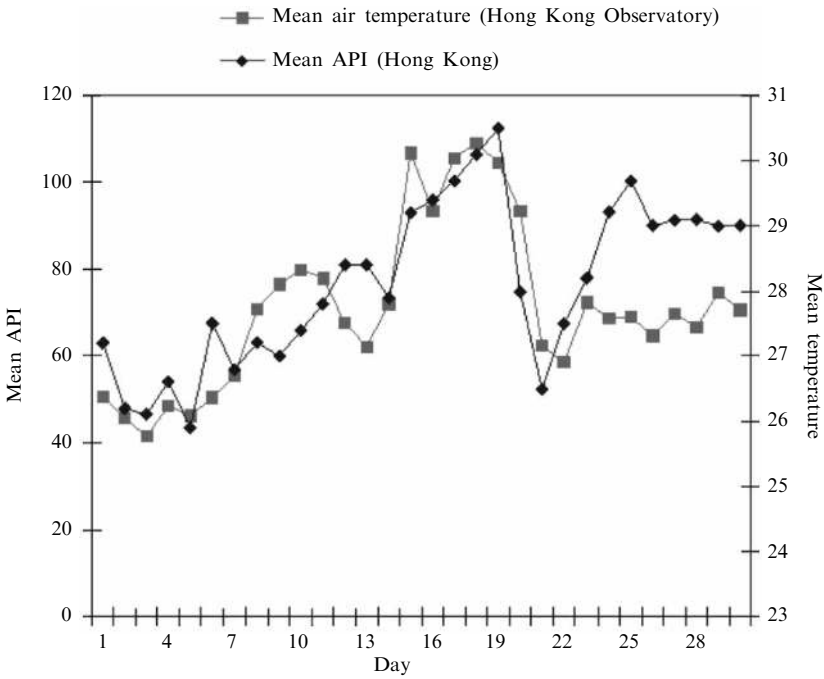


**Figure 9.** Daily pattern of air pollution indices (API) and mean temperature for September 2001 for Mongkok (temperature from the nearest climatic station at Kings Park) (sources: Environmental Protection Department, 2001 and The Hong Kong Observatory).

prevent pollutant dispersal and those associated with the UHI. This relationship has been observed in other subtropical cities: for example, in Mexico City (Klaus et al, 1999) where stale and polluted air accumulates at the heat island centre and in high-rise areas. This is because of convergence of air into the warm centre during the day as warm air rises, but this may be replaced at night by cool fresh air from adjacent uplands, if air-flow corridors are present.

Causeway Bay generally has the highest air pollution levels in Hong Kong thanks to extremely high-rise building geometry and the mountain backdrop in relation to the northerly, pollution-bearing winds from mainland China. Despite the tall buildings, giving a low SVF, an early heat island is evident on the images (colour plate 3, page 51). Air pollution levels are highest in the winter dry season, when the dust-bearing and pollution-bearing northerly winds are trapped in the flat coastal plain of Hong Kong Island. Natural fresh air corridors along ridges and valleys, extending from high mountains inland, down to the coast, and having the potential to moderate the build-up of air pollution and the UHI with cooler fresh air at night, are blocked by the transversely oriented tall buildings of Causeway Bay (A on colour plate 3).

The study also suggests that local factors of topography and urban morphology in relation to sun angle and azimuth are as influential as the surface type in controlling the amount of radiation received. Thus within the low-vegetated areas (that is, VD is kept constant) northwest Mongkok and ShamShuiPo, having streets oriented northwest – southeast are much warmer by up to 6°C than the rest of Mongkok whose streets run roughly north – south (figure 5). With a sun angle of 52° and azimuth of 127° at the image time, those street canyons oriented northwest – southeast are in direct sunlight because the solar direction is parallel to them. Other-oriented high-rise areas experience an early morning lag in heating thanks to shadow and are cooler (for example, south Mongkok and Causeway Bay). Additionally, the differential heating due to

aspect is strikingly evident on mountain slopes on all Landsat thermal images of Hong Kong. The east–west orientation of street canyons parallel to the footslope contour and transverse to the sun azimuth, especially in the high-rise districts of Causeway Bay and Central/Western, further blocks solar penetration to street level and delays heating.

Despite limitations of the image time with respect to heat island development, significant spatial relationships between image temperature and air quality parameters were established using the model data (Fung et al, 2003) for 10 am on the image date (table 4). For the thirty model pixels covering both rural and urban areas of Hong Kong (figure 1), positive relationships at the 5% significance level were established between $T_s$ and $NO_x$, volatile organic compounds, and PM2.5 (particulate matter less than 2.5 microns), and a negative relationship with ozone ($O_3$). However, such relationships may be expected because urban areas are known both to be warmer and to contain more emission sources. High correlations observed for the seven urban districts were more surprising thanks to a smaller overall range among the parameters. The lack of relationship between $T_s$ and $O_3$ may be explained by the fact that $O_3$ is scavenged by NO in urban areas by photochemical processes, particularly because temperatures at the image time are significantly high: above the approximately 22°C required (Dwyer et al, 1992) for photochemical reactions.

The lower correlations observed between biomass (VD) and air quality parameters may be affected largely by the radically different spatial scales of urban vegetation and air quality parameters, and this invokes a need for greater understanding of the modifiable areal unit problem in spatial data analysis (Fotheringham and Wong, 1991).

**Conclusion**

Lack of development space in Hong Kong thanks to the steep terrain does not permit the inclusion of much urban greenery (Jin, 1989). Therefore, strategic planning taking account of the natural topographic setting in relation to climatic patterns and building layouts is important in future development or renewal projects. At the hottest time of year in Hong Kong the sun passes directly overhead during the day. This is similar to the situation in Singapore where Nichol (1996) showed that the thermal effects of building geometry according to the sun angle and azimuth, are particularly evident on Landsat images. The Singapore study confirmed the effectiveness of the city's planning strategies in minimising north–south building orientations, especially for high-rise blocks. The cooling effects of planting campaigns, including the strategy of appropriate tree planting at the short, exposed (easterly and westerly) ends of buildings were especially evident on the images. The same strategy could be used in Hong Kong, especially as urban renewal takes place in flat areas of Kowloon such as Mongkok and ShamShuiPo. In mountain footslope areas, buildings at the downstream ends of valleys should not block fresh air corridors originating in cooler mountains inland. Because of the lack of public green space and pavement plantings in Hong Kong, small pockets of biomass which are purposely landscaped or have escaped development are especially important for their higher UEQ and many people use them (figure 7). Thus the 4 m spatial resolution of IKONOS and the sensitivity of the VD parameter to differing amounts of biomass permit small pockets of treed areas to be mapped as having higher UEQ than surrounding areas, and higher than grassed areas. For example, the surface temperature of the park (figure 8) is 6–7°C cooler than surrounding areas. Thus combination of the IKONOS image with the Landsat thermal data adds greater precision to UEQ assessment by remote sensing.

Extensive areas of low UEQ which are identified in this study as being vegetated but warm, including open grassy areas, could be improved by watering to promote

cooling by evapo-transpiration, as well as the addition of treed borders and their configuration into green, fresh air corridors in the urban area. Additionally, efforts should be made to plant trees on reclaimed land areas around the coast to reduce the SVF and mitigate intense surface heating. The resolve of the Hong Kong government to reduce building densities and to improve the living environment following from the SARS epidemic should mean less competition between trees and real estate.

The research described here makes a significant advance over previous attempts (Emmanuel, 1997; Fung and Siu, 2001) to use remotely sensed data as an index of urban environmental quality, which have used only one nonquantified parameter, the presence or absence of biomass. Moreover, previous work has been limited to low-resolution and medium-resolution sensors from Landsat MSS (80 m) (Emmanuel, 1997) and TM (30 m) (Fung and Siu, 2001). The use of IKONOS multispectral imagery with high spatial and radiometric resolution permits quantification of biomass amount at the detailed level of the individual city block, street, or building. Furthermore, its combination with thermal data provides an integrated UEQ index enabling the detailed measurement of spatial variations and thus comparisons between individual urban entities. The air quality model data used here to establish a relationship between image-based parameters and air quality may be superseded by the higher resolution (250 m and 500 m) aerosol data of the Moderate Resolution Imaging Spectroradiometer (MODIS) sensor, to give a more compatible spatial resolution for UEQ mapping, and in an image format which can provide a third image-based parameter for interactive assessment of UEQ.

**Acknowledgements.** The authors would like to acknowledge CERG Grant B-Q611 from the government of Hong Kong to the Hong Kong Polytechnic University, which funded this research.

**References**

Akbari H, Rosenfeld A H, Taha H, 1990, "Summer heat islands, urban trees and white surfaces" *ASHRAE Transactions* (American Society of Heating, Refrigerating, and Air-Conditioning Engineers) **96**(1) 1381 – 1388

Artis D A, Carnahan W H, 1982, "Survey of emissivity variability in thermography of urban areas" *Remote Sensing of the Environment* **12** 313 – 329

Barnsley M J, Barr S L, 1996, "Determining urban land use from satellite sensor images using kernel-based spatial reclassification" *Photogrammetric Engineering and Remote Sensing* **62** 949 – 958

Ben-Dor E, Saaroni H, 1997, "Airborne video thermal radiometry as a tool for monitoring the micro-scale structure of the urban heat island" *International Journal of Remote Sensing* **18** 3039 – 3053

Carlson T N, Boland F E, 1978, "Analysis of urban-rural canopy using a surface heat flux temperature model" *Journal of Applied Meteorology* **17** 998 – 1013

Colwell J E, 1974, "Grass canopy bi-directional spectral reflectance", in *Proceedings of 9th International Symposium on Remote Sensing of Environment* Ann Arbor, MI, pp 1061 – 1085

Curran P, 1980, "Multispectral remote sensing of vegetation amount" *Progress in Physical Geography* **4** 315 – 341

Curran P, 1983, "Estimating green LAI from multispectral aerial photography" *Photogrammetric Engineering and Remote Sensing* **49** 1709 – 1720

Dwyer J F, MacPherson G E, Schroeder H W, Rowntree R A, 1992, "Assessing the benefits and costs of the urban forest" *Journal of Arboriculture* **18**(5) 227 – 234

Emmanuel, 1997, "Urban vegetational change as an indicator of demographic trends in cities: the case of Detroit" *Environment and Planning B: Planning and Design* **24** 415 – 426

Environmental Protection Department, 2004 *Air Quality in Hong Kong 2003* (The Government of Hong Kong, Hong Kong)

Fotheringham A S, Wong D S W, 1991, "The modifiable areal unit problem in multivariate statistical analysis" *Environment and Planning A* **23** 1025 – 1044

Fung T, Siu W L, 2001, "A study of green space and its changes in Hong Kong using NDVI" *Geographical and Environmental Modelling* **5**(2) 111 – 122

Fung C, Yu L, Leung K, Chang A, Lau H C, 2003, "Testing a real-time air quality simulation system for Hong Kong", paper presented at the Air and Waste Management Association, 96th Annual Conference, 22-26 June, San Diego, TX; copy available from the authors

Gallo K P, McNab A L, Karl T R, Brown J F, Hood J J, Tarpley J D, 1993a, "The use of NOAA AVHRR data for assessment of the urban heat island effect" *Applied Meteorology* **32** 899 – 908

Gallo K P, McNab A L, Karl T R, Brown J F, Hood J J, Tarpley J D, 1993b, "Use of a vegetation index for assessment of the urban heat island effect" *International Journal of Remote Sensing* **14** 2223 – 2230

Gao J, Skillcorn D, 1998, "Capability of SPOT XS data in producing detailed land cover maps at the urban-rural periphery" *International Journal of Remote Sensing* **19** 2877 – 2891

Hanley T A, 1978, "A comparison of line-intercept and quadrat estimation methods of determining shrub canopy coverage" *Journal of Rangeland Management* **31** 60 – 62

Jin C Y, 1989, "The distribution and configuration of tree cover in urban Hong Kong" *GeoJournal* **18** 175 – 188

Klaus D, Jauregui E, Poth A, Stein G, Voss M, 1999, "Regular circulation structures in the tropical basin of Mexico City as a consequence of the heat island effect" *Erdkunde* **53** 231 – 243

Lawrence R L, Ripple W J, 1998, "Comparisons among vegetation indices and bandwise regression in a highly disturbed heterogeneous landscape: Mount St Helens, Washington *Remote Sensing of Environment* **64** 90 – 102

Lo C P, Quattrochi D A, Luvall J C, 1997, "Application of high resolution thermal infra-red remote sensing and GIS to assess the urban heat island effect" *International Journal of Remote Sensing* **18** 287 – 304

Nichol J E, 1994, "A GIS based approach to microclimate monitoring in Singapore's high rise housing estates" *Photogrammetric Engineering and Remote Sensing* **60** 1225 – 1232

Nichol J E, 1996, "Analysis of the urban thermal environment with LANDSAT data" *Environment and Planning B: Planning and Design* **23** 733 – 747

Nichol J E, 2005, "Remote sensing of urban heat islands by day and night" *Photogrammetric Engineering and Remote Sensing* **71** 613 – 621

Nichol J E, Lee C M, 2005, "Urban vegetation monitoring in Hong Kong using high resolution multispectral images" *International Journal of Remote Sensing* **26** 903 – 919

Nowak D J, Rowntree R A, McPherson E G, Sissini S M, Kerkmann E R, Stevens J C, 1996, "Measuring and analyzing urban tree cover" *Landscape and Urban Planning* **36** 49 – 57

*South China Morning Post* 2002, "High rises send temperatures soaring", 23 September, City, page 1

Spronken-Smith R A, Oke T R, 1998, "The thermal regime of urban parks in two cities with different summer climates" *International Journal of Remote Sensing* **19** 2085 – 2104

Weng Q, 2001, "A remote sensing-GIS evaluation of urban expansion and its impact on surface temperature in the Zhujiang Delta, China" *International Journal of Remote Sensing* **22** 1999 – 2014

## Appendix

## Conversion of ETM+ thermal image to surface temperature ($T_s$)

### DN to radiance

Conversion of the image digital number (DN) values to spectral radiance is carried out using the gain and offset values given in the image header file:

$$L_\lambda = \frac{L_{max} - L_{min}}{Q_{calmax} - Q_{calmin}} (Q_{cal} - Q_{calmin}) + L_{min}, \quad \text{(A1)}$$

where $Q_{calmin} = 1$, $Q_{calmax} = 255$, and $Q_{cal} = \text{DN}$; $L_{min}$ and $L_{max}$ are the spectral radiance for band 6 at DN = 0, and DN = 235.

### Spectral radiance to black body temperature

The ETM+ thermal band data can be converted from spectral radiance to black body temperature, which assumes that surface emissivity = 1:

$$T = K_2 \Big/ \ln\left(\frac{K_1}{L_\lambda + 1}\right), \quad \text{(A2)}$$

where

$T$ is the effective at-satellite temperature in K;
$K_1$ is calibration constant 1 in W m$^{-2}$ sr$^{-1}$ (666.09);
$K_2$ is calibration constant 2 in K (1282.7);
$L_\lambda$ is the spectral radiance in W m$^{-2}$ sr$^{-1}$.

### Emissivity correction

Geometric correction to the Hong Kong Grid coordinate system was performed for the IKONOS and ETM+ images using a third-order, cubic polynomial regression equation derived from thirty-four and eighteen ground control points, respectively. The four IKONOS bands were then classified into three main land-cover classes (vegetation, nonvegetation, and water) using a supervised classification. Corrections for emissivity differences were then carried out by land-cover type by ratioing the $T$ image from ETM+ with the classified image from IKONOS in which the pixel values for the land-cover class were replaced with the corresponding emissivity value (Nichol, 1994; 1996). Thus the emissivity-corrected surface temperature ($T_s$) is derived from (Artis and Carnahan, 1982):

$$T_s = T \Big/ \left(1 + \frac{\lambda T}{\alpha} \ln \varepsilon\right), \quad \text{(A3)}$$

where

$\lambda$ is the wavelength of emitted radiance;
$\alpha = hc/K$ ($1.438 \times 10^{-2}$ m K);
h is Planck's constant ($6.26 \times 10^{-34}$ J s);
c is the velocity of light ($2.998 \times 10^{8}$ m s$^{-1}$);
K is Bolzmann's constant ($1.38 \times 10^{-23}$ J K$^{-1}$).

The following surface emissivity ($\varepsilon$) values were used:

nonvegetation (baresoil/concrete/sand): $\varepsilon = 0.92$
vegetation: $\varepsilon = 0.96$
water: $\varepsilon = 0.99$.

The emissivity correction procedure has the effect of reducing the original 60 m pixel size of the thermal data to 4 m because of fusion with the land-cover map resulting from classifying the 4 m pixels of IKONOS. The effect is not equivalent to increasing the spatial resolution of the thermal data, but the resolution is increased to the extent to which the emissivity differences of land-cover materials affect surface temperature.

**Atmospheric correction**

The $T_s$ images were atmospherically corrected by comparison with sea surface temperature data from the Hong Kong Observatory (HKO), which, although taken approximately 1 m below the surface, were observed to be within $+/-0.5^{\circ}$C of the satellite-observed 'skin' surface temperature. Thus for the ETM+ image 10 DN values were added before conversion to radiance, having the effect of raising $T_s$ values by 5°C. This resulted in $T_s$ values for the sea surface being adjusted to the HKO value of 29°C, and all other image values being so adjusted.